Infrared Microspectroscopy and Imaging

Lisa M. Miller
National Synchrotron Light Source
Brookhaven National Laboratory
lmiller@bnl.gov

INTRODUCTION

Unlike many x-ray based spectroscopies, which were made possible by the advent of synchrotron radiation, infrared (IR) spectroscopy has been used for many years without the benefits of a synchrotron source. Commercial IR spectrometers are equipped with conventional thermal (globar) sources that provide IR power that is comparable to the IR radiation emitted from a synchrotron. However, the primary advantage of synchrotron IR light is its brightness (defined as the photon flux or power emitted per source area and solid angle), which is 100-1000 times greater from a synchrotron source (Duncan and Williams, 1983). This brightness advantage is not because the synchrotron produces more power, but because the effective source size is small and the light is emitted into a narrow range of angles.

High brightness is desirable for any measurement with a limited "throughput", meaning either a small sample area, the requirement for a narrow beam, or a combination of both. Microspectroscopy is perhaps the best-known example of a measurement with low throughput, and the synchrotron source is well suited to this technique.

IR microscopes equipped with conventional IR sources have been available for nearly 20 years and have proven extremely valuable for resolving the chemical components in a wide range of materials, including numerous plant and animal tissue, polymers and laminates, geological samples, etc. However, the long wavelengths of IR radiation limit the spatial resolution that

can be achieved. When considering the available spatial resolution, two issues should be taken into account. The first consideration is the acceptable signal-to-noise ratio (S/N), which decreases as apertures are closed to confine the IR beam to smaller areas. The second issue is diffraction. Existing instruments using a conventional IR source encounter a S/N limitation when apertures confine the IR to an area of 20-30 μm in diameter.

The high brightness of the synchrotron source allows smaller regions to be probed with acceptable S/N (Reffner et al., 1995; Carr et al., 1995). Indeed, aperture settings smaller than the wavelength of light can be used; though in this case, diffraction controls the available spatial resolution (Carr and Williams, 1997). Thus for a specimen with an absorbance feature in the C-H stretch region (e.g. 3000 cm^{-1}), the diffraction-limited spatial resolution is approximately 3.3 μm (10^4/3000 cm^{-1}). This improvement in spatial resolution achieved by using a synchrotron IR source has only been realized recently, and many applications are still in their infancy.

INSTRUMENTATION

Infrared beamlines

IR light passes easily through air, so IR microscopes operate under ambient pressure conditions. However, water vapor and carbon dioxide (CO_2) absorption are frequently a nuisance, so a vacuum, dry-nitrogen, or dry-air environment are desired. Most infrared beamlines operate under low vacuum conditions (10^{-3} – 10^{-4} torr), and the high vacuum of the storage ring is isolated by a diamond window. Infrared beamlines are then terminated with a window (KBr, CsI, polyethylene) to isolate the beamline vacuum from the ambient pressure of the microscope.

Infrared microscopes

Infrared microscopes are commercially available from a number of companies worldwide. Very little modification needs to be made to adapt a commercial microscope for a synchrotron infrared source. From
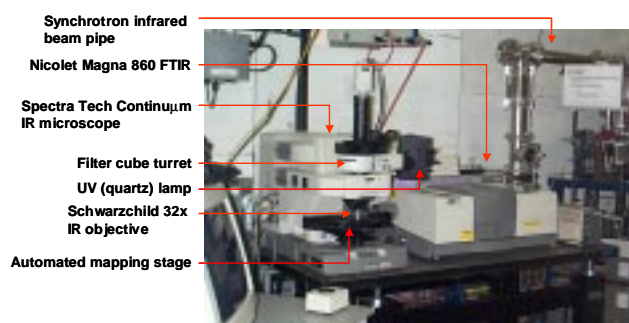

Synchrotron infrared beam pipe
Nicolet Magna 860 FTIR
Spectra Tech Continuμm IR microscope
Filter cube turret
UV (quartz) lamp
Schwarzchild 32x IR objective
Automated mapping stage

Figure 1. *Infrared microscope at Beamline U10B.*

the beamline, a collimated beam of IR light first enters the interferometer, which modulates the wavelength of light, and then passes into the IR microscope. Infrared microscopes are very much like a conventional visible light microscope, except all of the optics are mirrors (instead of lenses). This is done so that the broad wavelength range of IR light can pass through the system without being absorbed. Because of this design, modern IR microscopes operate very much like a visible light microscope for sample viewing. Because of their modern design, they are also equipped with a number of convenient methods for enhanced sample visualization. These include polarized light, fluorescence illumination, and differential interference contrast (DIC). The infrared microscope at Beamline U10B can be seen in **Figure 1**.

In addition to sample visualization, the IR light follows the same path as the sample illumination light, so that IR microspectroscopy can be performed on the sample at the center of the viewing field. The illumination area of the sample with IR light is determined by setting a mechanical aperture in the microscope. Many microscopes have dual apertures, so that the IR light is masked before and after the sample. A conventional globar source illuminates light into a ~100 μm area, so typical aperture settings are 20-100 μm. Conversely, the synchrotron IR light fills a 10-20 μm area only because of the small effective source size of the synchrotron. Thus, unlike a globar source that transmits very little light through a 10 μm aperture, >80% of the synchrotron IR light passes through the same size aperture (**Figure 2**).
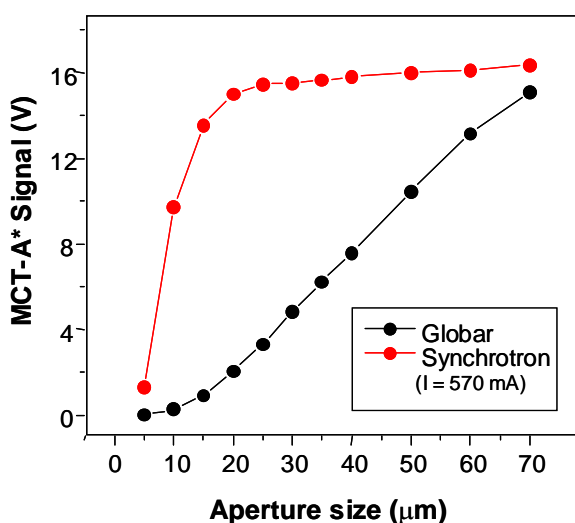

Figure 2. *Intensity of infrared light as a function of aperture size for the synchrotron versus conventional black body (globar) source.*
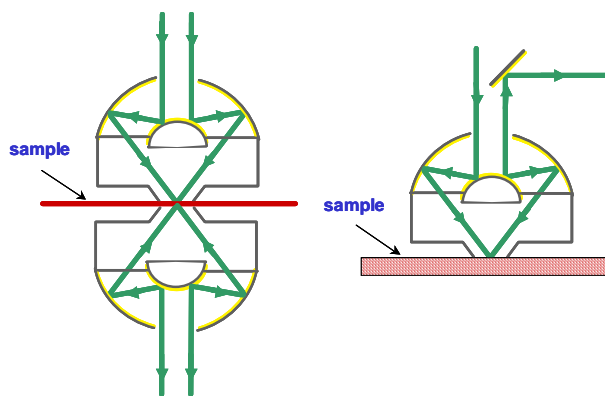

Figure 3. *Path of the IR beam in (left) transmission and (right) reflection modes.*

IR microscopes are generally designed with 2 paths from the sample to the detector: transmission and reflection (**Figure 3**). In the transmission mode, the IR light passes through the sample and is collected by a second IR objective that re-collimates the beam and sends it to the IR detector. In reflection mode, the IR light reflects off of the sample and passes back through the illuminating objective. In this configuration, approximately 40-50% of the incident IR light is blocked by a mirror that collects the reflected light. Thus, given the choice, transmission mode is preferred over reflection mode because of the increased incident flux on the sample.

IR microspectra are generally collected as (1) individual microspectra, or (2) part of a line or area map. For most IR microscope systems, the latter mode is automated with software control and a motorized microscope stage. Line and area maps are defined by an aperture size and a step size. Although data collection times vary widely as a function of aperture size and mode of data collection, typical IR microspectra take anywhere from 10-30 seconds (e.g. transmission mode, 10 mm square aperture) to 5-10 minutes (e.g. GI or ATR modes, see next section). Since area maps often take a number of hours to collect, they span more than one fill of the storage ring. In these cases, a mapped can be paused during the fill. If allowed to run, data points collected during the fill may or may not yield satisfactory data.

Infrared Detectors

Infrared microscopes are generally equipped with liquid nitrogen-cooled MCT detectors, which are sensitive from approximately 4000 – 650 cm^{-1}. MCT-A detectors have higher sensitivity (and S/N), but the frequency range is limited. MCT-B detectors have a reduced sensitivity, but can be used to ~500 cm^{-1}. Since

synchrotron IR light is available well into the far-infrared region, IR microscopes are now being modified for low frequency detectors (e.g. Cu-doped Ge, B-doped Si, bolometer). Since these detectors are generally large because they are cooled by liquid helium, they are mounted external to the IR microscope.

SAMPLE PREPARATION AND DATA COLLECTION

Sample preparation is perhaps the most critical part of a successful IR microspectroscopy experiment. Since there are a number of ways to use the IR microscope to collect microspectra, sample preparation can also be done in a variety of ways.

Transmission

The simplest way to collect IR microspectra is in transmission mode. In this mode, thin samples are generally needed. Although it is very sample-dependent, typical thicknesses for transmission measurements are 5-30 μm. Polymers, unmineralized biological tissues, and other organic materials are generally prepared with thicknesses of 10-15 μm. Minerals (biological and geological) are much more variable, depending on the type of mineral. Preparation of thin sections is usually done by embedding the sample and then cutting with a microtome. Embedding compounds are generally chosen to match the hardness of the sample. Since these compounds usually penetrate throughout the sample, care must be taken to choose a material that does not have IR absorption features that overlap those of the sample. For many biological tissues, paraffin is a good choice because most of its absorbance features are limited to the C-H stretch region (2800-3000 cm^{-1}). In some cases (e.g. many non-mineralized animal tissues), cryo-sectioning of unembedded materials can be done. Since an embedding medium is not used for cryo-sectioning, this is the method of choice for preparing thin sections if possible.

Once a thin section is cut, it is placed on an infrared-transparent material that is 1-2 mm thick. Common materials can be seen in Table 1. A list of suggested vendors for these materials can be found in the "Useful Websites" section.

Table 1	
Material	Transmission Range (cm^{-1})
CaF$_2$	4000 – 1100
BaF$_2$	4000 – 800
ZnS	4000 – 600
ZnSe	4000 – 650
KBr*	4000 – 400
diamond**	4000 – 50

*inexpensive but water soluble

**can be cost prohibitive

Reflection

The second most common way of collecting IR microspectra is in reflection mode. As mentioned above, it is less-preferred than transmission mode because up to half of the incident IR light is blocked by a mirror that collects the reflected light. Samples probed in reflection mode are most often (1) highly reflective samples, e.g. polymer coatings on a reflective substrate, (2) semi-reflective or polished samples that cannot be cut to thin sections, e.g. shells, bones, embedded materials that cannot be cut thin, or (3) microtomed thin sections that are placed on an IR-reflective substrate instead of an IR-transparent substrate.

For coatings on highly reflective substrates, the thickness of the coating is generally on the order of 1 – 10 μm. For sub-micron thick coatings, grazing incidence IR microspectroscopy is often used because it is a more surface-sensitive technique (see next section). Semi-reflective and polished samples are also probed in reflection mode. Since the S/N of the spectra relies strongly on collection of the reflected light back into the IR objective, it is important that these samples have a smooth and flat surface. Uneven surfaces can scatter light, reducing the collection efficiency. Samples that have surfaces that are not flat can be mounted into a micro-goiniometer to adjust the tilt of the sample with respect to the incoming beam. Even simpler, samples can also be pressed into a small sphere of putty so that the sample surface is parallel to the microscope stage.

Recently, reflection mode has become more popular for probing microtomed thin sections that have been placed on IR-reflective substrates. For these experiments, the IR beam penetrates through the sample, reflects off of the substrate, and the reflected beam then passes back through the sample again. Since the beam passes through the sample twice, the result is a "double-absorption" spectrum. For this reason, the thin sections should be cut to ~1/2 the thickness used for a transmission measurement. The primary reason for using reflection mode for thin sections is the cost-efficiency of the method. In general, the cost of a glass microscope slide with an IR-reflective coating (e.g.

Low-e slides from Kevley Technologies) is approximately $1/50^{th}$ the cost of an IR-transparent substrate disk (BaF_2 or CaF_2). In addition, the glass slides are larger and easier to handle than the conventional IR-transparent substrates. However, the use of IR-reflective substrates does come at a cost to the IR data collection process and even spectral quality. As noted above, the incident flux in reflection mode is reduced by almost 50% compared to transmission mode. So data collection generally takes longer to achieve sufficient S/N. In addition, any inhomogeneities in the thin section can cause oscillations in the background of the IR spectra. Thus, care must be taken with sample preparation, and only certain (generally homogeneous) samples work well in this mode.

Grazing Incidence

Grazing incidence (GI) mode is a surface-sensitive technique that is often used for very thin films on highly reflective substrates. GI involves the use of a Schwarzchild IR objective that contains a beam "mask" that transmits only the grazing incidence rays onto the sample. Typical GI objectives transmit light grazing light at angles between ~65 - 80°. By using GI mode, the penetration depth of the light is reduced, so the surface of the material is preferentially selected. The major drawback to GI mode is the reduction in flux on the sample, due to the beam mask. Although the synchrotron source dramatically improves the transmission through the mask, the incident flux is generally reduced by up to 40-65% from the standard reflection mode. However, this is considerably better than the conventional globar source, which loses up to 90% of the throughput in GI mode. Due to the inherently low throughput of the technique, sample preparation for GI mode is extremely critical. Samples are generally thin films or coatings on highly reflective substrates. Films that are typically < 1μm thick can benefit from GI mode. Thicker films can be probed with conventional reflection IRMS. Substrates are commonly polished metallic, semiconductor, or silicon surfaces, but any IR-reflective substrate can be used. The most important feature of the substrate is that it is highly polished to optimize the reflectivity of the IR light.

Attenuated Total Reflection (ATR)

For samples that (1) are not reflective, and (2) cannot be cut into thin sections, ATR mode can be used. An ATR objective is a Schwarzchild IR objective that contains an ATR crystal made of an IR transparent material such as ZnSe, Ge, or diamond (**Figure 4**). Light entering the ATR objective is filtered with a beam
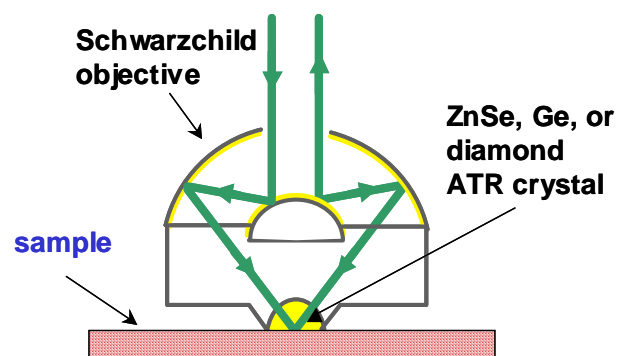

Figure 4. Path of the IR beam through an ATR objective.

mask (similar to GI mode) so that only grazing incidence beams are transmitted. These rays then pass into the ATR crystal where they are totally internally reflected and collected in reflection mode. In order to probe the sample, the ATR crystal must be in contact with it. This way, the light that is normally reflected inside of the ATR crystal "leaks out" and is absorbed by the sample, where the penetration depth of the light is on the order of the wavelength (e.g. 10 μm at 1000 cm^{-1}). The result is a "reflection loss" absorbance spectrum of the sample that is then corrected for penetration depth as a function of wavelength. As with GI mode, the mask and ATR crystal cause a reduction of the incident flux on the sample by 40 – 65% from the standard reflection mode. However this loss is much less pronounced compared to the conventional globar source. There is very little sample preparation for ATR, however not all samples are ATR-compatible. Since the ATR crystal must come in contact with the sample, the sample must be firm, and/or mounted on a stiff substrate. Soft and/or non-resilient samples may be damaged by contact with the ATR crystal. Moreover, may samples (e.g. many biological tissues) leave a residue on the ATR crystal that must be cleaned off prior to collecting the next spectrum. Since the microscope stage must be raised and lowered between sample data points, automated mapping of the sample is prohibitive. Finally, the spectral range for data collection is limited by the transmission properties of the ATR crystal in the objective, which must be chosen accordingly.

DATA ANALYSIS

Spectral interpretation is often a highly subjective process, a fact that is made worse when one considers the many hundreds of spectra that are often acquired from a single sample. These issues were first realized with the development of IR focal plane array detectors, which enable individual spectra to be collected at

each pixel simultaneously, dramatically increasing the data acquisition rate (Lewis et al., 1995; Colarusso et al., 1998). To date, these detectors have not been used with synchrotron sources. To address these concerns, pattern recognition techniques are currently being developed and applied to IR data. These methods help to remove subjectivity and allow realistic processing of large data sets.

The choice of techniques is highly dependent upon the sample, but common methods are described here. IR microscopes are equipped with basic data analysis software, but their capabilities are often limited. More comprehensive software packages are also available. Vendors for common data analysis packages are listed in the appendix.

Peak Height / Peak Area

Perhaps the most straightforward method of data analysis is the mapping of specific functional group intensities and frequencies. Analysis of absorbance peak heights and/or peak areas provide a measure of component concentration. Provided that individual components can be uniquely identified, measuring peak heights and/or areas is the most straightforward way of identifying its location and concentration. In order to account for variations in sample thickness (within a single sample and/or between multiple samples), peak height/area ratios are frequently used.

Second derivatives and deconvolution

Although these methods requires data with excellent S/N ratios (which is a key benefit of using synchrotron light), second derivatives and Fourier self-deconvolution (FSD) are a powerful ways to determine peak frequencies under broad absorption contours, e.g.

the Amide I band in proteins (Byler and Susi, 1986; Susi and Byler, 1983). In addition, second derivative and FSD spectra can be combined with correlation and/or cluster analysis to analyze IR maps (see below).

Correlation analysis

Correlation analysis involves the comparison of a "standard" IR spectrum to the remainder of the spectra in a map. For example, this technique is often used to identify contaminants in a sample. In correlation analysis, a least-squares fit is performed between each data point in the "standard" spectrum and the "unknown" spectrum. A correlation value between 0 and 1 is calculated, where a perfect fit is represented by a value of 1.0. Correlation analysis is commonly performed on either original or second derivative spectra.

Cluster analysis & other multivariate techniques

Due to the complexity of many samples, more sophisticated methods of data analysis are now being used. Cluster analysis is a technique which groups (or clusters) IR spectra in a map based on similarity with other spectra in the same map (see **Figure 5**). Cluster analysis can be done "unsupervised", because the comparisons are made mathematically, i.e. it does not require the user to have any knowledge of the sample composition. Of course once cluster analysis is performed, a spectral average of each cluster is generated and must be interpreted. In addition to cluster analysis, other multivariate techniques can be used including linear discriminate analysis (LDA) and principle component analysis (PCA). These methods of analysis are described further in (Jackson and Mantsch, 1999).

Infrared Beamline Programs at the NSLS

Beamline	Program	PRT Membership	Contact Person
U2A	geophysics, materials at extreme pressures and microspectroscopy	Carnegie Institute of Washington	Rus Hemley
U2B	biological applications and microspectroscopy	Albert Einstein College of Medicine	Mark Chance
U4-IR	far IR spectroscopy, microspectroscopy, surface physics and chemistry	NSLS, BNL	Larry Carr
U10B	near-, mid- and far- IR microspectroscopy	NSLS, BNL Canadian Light Source	Lisa Miller Emil Hallin

EXAMPLES

Plaque Identification in Alzheimer's Disease

L.M. Miller,[1] A. Kis,[2] A. Radenovic,[2] L. Forro,[2] and J. Miklossy[3]

[1]*Brookhaven National Laboratory*
[2]*Swiss Federal Institute of Technology*
[3]*Temple University*

Alzheimer's diseased brain is characterized by the presence of amyloid plaques that are thought to kill neurons in the brain. These plaques consist of aggregates of misfolded β-amyloid protein. To date, the *in situ* structure of this misfolded protein is unclear and the mechanism by which the plaques form and damage surrounding nerve cells has yet to be elucidated. By combining fluorescence microscopy and synchrotron IRMS, the plaques can be identified in the tissue and the *in situ* structure of the misfolded β-amyloid protein can be determined.

β-amyloid plaques in brain stains positive with Thioflavin S and can be identified in brain tissue by their green fluorescence. **Figure 5A** illustrates the β-amyloid deposition in the leptomeningeal and cortical blood vessels in the brain. IR spectra from the amyloid (green) and normal (dark) regions of the tissue can be seen in **Figure 5**. The Amide I band (1700 – 1600 cm^{-1}), which arises from the C=O stretching vibration of a protein backbone, is very sensitive to protein secondary structure (Byler and Susi, 1986). When comparing the Amide I spectral features of the amyloid versus normal brain tissue, dramatic differences are observed, indicating significant differences in protein structure. Specifically, the Amide I band of the normal tissue ex-

hibits a single peak near 1650 cm^{-1}, representing an α-helical protein environment. In contrast, the Amide I band of the amyloid plaque contains two peaks, indicating a mixture of secondary structures in the plaque region. In addition to the α-helical component near 1650 cm^{-1}, an intense second peak is apparent near 1630 cm^{-1}, which is indicative of a β-sheet protein structure. Thus, the formation of β-amyloid plaque in the brain is associated with a change in protein secondary structure from a-helical to β-sheet, which likely leads to aggregation of the misfolded protein. An infrared image of the β-amyloid deposits was generated through cluster analysis of the Amide I region (**Figure 5C**). Four clusters were identified, each having unique IR spectra. By matching the fluorescence image pixels (**Figure 5B**) with the cluster analysis image, the highest correlation with the Thioflavin-S fluorescence was found with the orange cluster. The average IR spectrum of the orange cluster confirms the presence of misfolded (β-sheet) protein at these locations. Future studies will use other IR spectral features to study the health an integrity of the neurons surrounding the
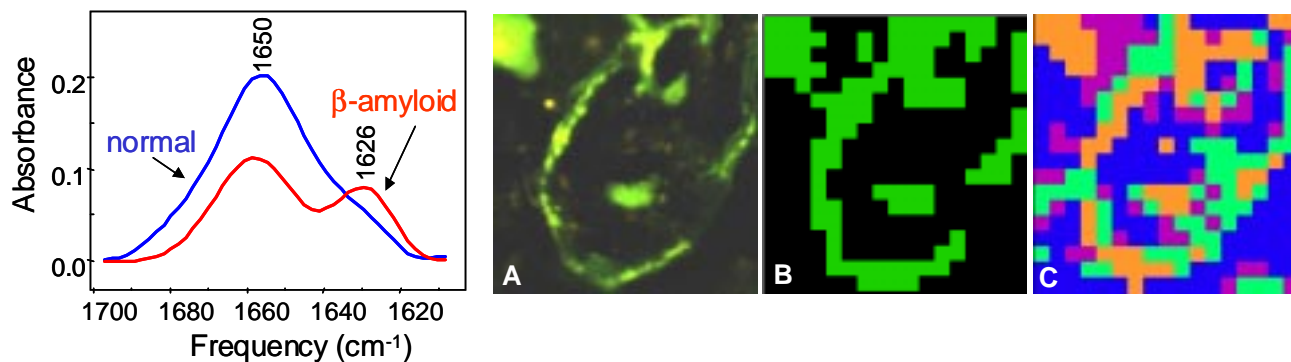

Figure 5. *(Left) IR spectra of normal (dark) and β-amyloid (green) regions. (A) Fluorescence image of AD brain tissue stained with Thioflavin S. Green areas indicate the presence of β-amyloid. (B) Pixelated image of (A), where green areas indicate Thioflavin S fluorescence and black areas are unlabeled. (C) IR cluster analysis of the Amide I band. Four clusters were identified, each having unique IR spectra. By comparing (B) and (C), cluster 4 (orange) has the highest correlation with the Thioflavin-S fluorescence.*

misfolded amyloid plaques. In addition, the combination of fluorescence microscopy and IRMS are being used to examine protein structure in regions of non-neuronal tissue (e.g. pancreas) that label positive for Thioflavin-S. These comparisons will allow the direct correlation of the structure of amyloid plaques in the brain with amyloid deposition in other tissues, and may lead to a method for early diagnosis of Alzheimer's disease.

. . . .

Examining the Earliest Phases of Bone Mineralization

M.J. Glimcher[1] and L.M. Miller[2]

[1]*Children's Hospital, Harvard University*
[2]*Brookhaven National Laboratory*

Field of research: biological/geological
Mode of data collection: attenuated total reflection (ATR)
Data analysis: peak areas, curve-fitting
Sample preparation: None — bone tissues were examined in their intact, hydrated state.

Bone is composed of protein and mineral components. It is known that collagen deposition and cross-linking are necessary precursors to mineralization, but the method by which the collagen matrix "seeds" crystallization is unclear. Mature bone mineral is described as highly-substituted hydroxyapatite, but there is a long-standing controversy about the nature of the earliest state of bone mineral. Two primary candidates for new bone mineral are amorphous calcium phosphate (ACP) and octacalcium phosphate (OCP). The formation of either of these phases of solid calcium phosphate, however, would be unstable and rapidly convert to hydroxyapatite. Thus, identifying the first bone mineral crystals is a difficult task.

Intramuscular herring bones have unique mineral-ization properties; one end of the bone is completely mineralized and the opposite end of the bone is non-mineralized. In this study, attenuated total reflection infrared microspectroscopy is used to examine the mineral composition of the herring bone near the point where mineralization begins. In order to "capture" the (unstable) earliest mineralization phase, a diamond Schwarzchild ATR objective is used for examining the whole bone, without the need to embed and section the sample. The combination of a diamond ATR crystal and an MCT-B detector permits analysis of the important ν_4 phosphate contour for the first time.

Using a 10x10 μm aperture, infrared spectra are collected in 10 μm steps along the length of the bone. **Figure 6** illustrates that the $\nu_{1,3}$ (900-1200 cm^{-1}) and ν_4 (500-650 cm^{-1}) phosphate contours increases in intensity along the length of the bone, indicating an increase in bone mineralization. At the lowest mineralization observed in this map (~2% of maximum), the phosphate contour slightly resembles that of poorly crystalline biological apatite. However, clear differences exist, notably an intense feature at ~520 cm^{-1}, which has been attributed to HPO$_4^{2-}$ in the crystal lattice. In addition, the normal ν_4 apatitic phosphate modes are shifted to lower frequency, suggesting a unique phosphate environment in these early mineralization stages.
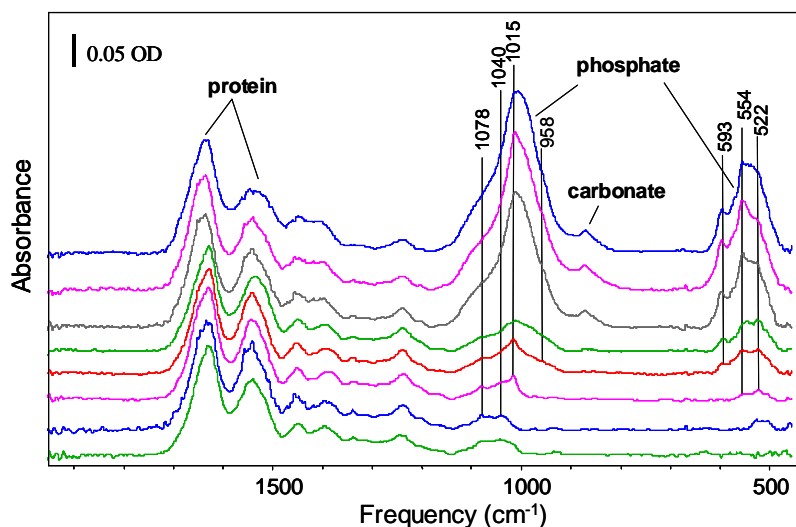

Figure 6. Infrared spectra of intact herring bone using ATR-IR microspectroscopy. Data were collected from one end of the bone to the other, which corresponds to the least and most mineralized regions, respectively. The spectra shown above were collected in 10 micron steps. of All spectra are normalized to the Amide I (protein) content to illustrate changes in mineralization.

Quality Control and Contaminant Identification for the Microelectronics Industry

T.J. Tague[1] and L.Miller[2]

[1]*Bruker Instruments*
[2]*Brookhaven National Laboratory*

The microelectronics industry continues to be focused on miniaturization of integrated components on silicon wafers. For the integration of microcomponents to be effective, the wafer must be clean to the parts per billion level (Fogarassy et al., 1987). After component integration takes place, individual components can suffer damage when conducting surface contaminants are present. Typically, quality control is performed at many steps in the manufacturing process to ensure that the product is free of contaminants. When contaminants are found, it is vital that chemical characterization of the particles takes place to determine the source of contamination.
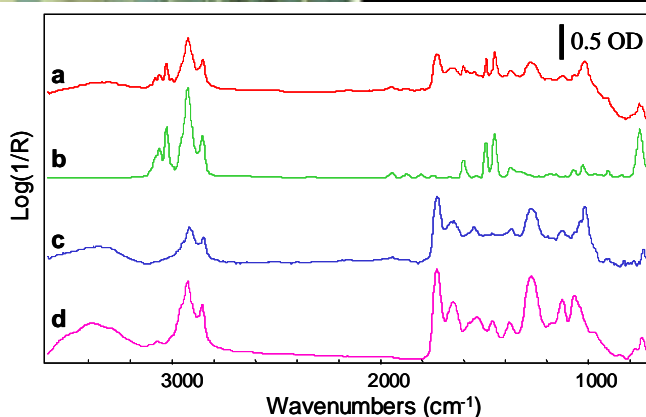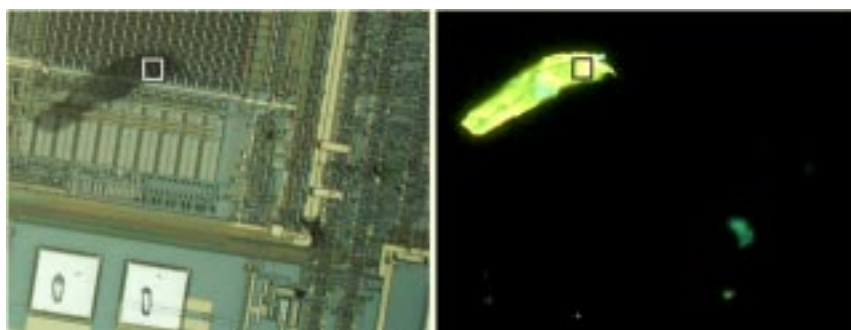
Field of research: materials and polymer science, industrial
Mode of data collection: reflection with combined fluorescence microscopy
Data analysis: spectral database fitting
Sample preparation: None — circuit board was examined in its natural state.

Currently, there are no satisfactory techniques for performing quality control on semiconductor wafers and circuit boards. Typically, an optical microscope is used to scan for contaminant particles. This can be a tedious process and is particularly difficult when investigating integrated circuits. Under normal illumination, it is difficult to discern the presence of dust and other small contaminant particles within an integrated circuit (**Figure 7**). In contrast, fluorescence illumination with ultraviolet light cloaks the non-fluorescing components, making it easy to identify contaminant particles. Once identified, an aperture is set to mask a specific particle and IRMS is used to characterize the chemical makeup of that contaminant (Chyan et al., 1997b; Chyan et al., 1997a).

Infrared analysis of one of the contaminant particles in **Figure 7** reveals the presence of low molecular weight polystyrene (**Figure 7a**). **Figure 7b** shows a reference spectrum of polystyrene (molecular weight 800) and **7c** shows the result of mathematically subtracting the polystyrene spectrum from the raw spectrum. Finally, **Figure 7d** shows a reference spectrum of an alkyd urea resin, which closely matches the subtraction result found in **Figure 7c**. Thus, the identification of the these contaminants allows for precise identification of their origins in the manufacturing process.

Figure 7. *Optical images of an integrated wafer under (top left) normal reflection illumination, and (top right) ultraviolet fluorescence illumination. (Bottom) Infrared spectra collected from (a) the highlighted particle on the integrated wafer, and (b) an 800 MW polystyrene from the Hummel Polymer Reference Library (Nicolet Instrument Corp.). (c) Infrared spectrum resulting from the subtraction of the polystyrene reference spectrum from the raw spectrum. (d) Infrared spectrum of an alkyd urea resin, also from the Hummel Polymer Library. For each IR spectrum of the contaminant, 128 scans were collected in reflection mode at 4 cm^{-1} resolution using a 10 x10 μm square aperture and an MCT-A detector.*

Corrosion Studies of Thin Metal Oxides

V.Srinivasamurthi,[1] G.Adzic,[1] L.Miller,[1] N.Marinkovic,[2] H.Isaacs,[1] S.Mukerjee[3]

[1]*Brookhaven National Laboratory*
[2]*Canadian Light Source*
[3]*Northeastern University*

Field of research: materials, surface science
Mode of data collection: grazing incidence
Data analysis: peak position and area integration
Sample preparation: Oxide films were electrochemically grown on metal substrates and dried.

The formation of oxide layers on metal surfaces is important in the corrosion process. Iron oxides have attracted a great deal of attention lately, where much of the recent work has focused on the passivity of Fe in alkaline solutions and borate buffers. A number of *ex situ* and *in situ* techniques using XANES have been used and has led to a fairly good understanding of the electrochemistry taking place. However, oxide films can also be grown at a high pH, where the mechanisms of formation and the nature of these layers are not yet clear.
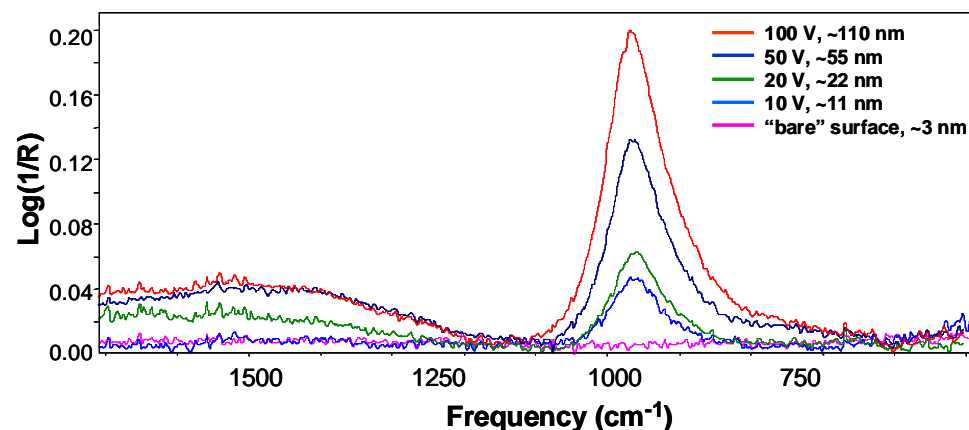
IR spectroscopy can distinguish oxide films by the frequency of the metal-oxygen stretching and bending vibrations. By using grazing incidence methods, very thin films can be detected on surfaces. Figure X shows the IR spectra resulting from the growth of the oxide on an Al sample at 10mA/cm^2 to different potentials. Each of these oxides were grown at a certain current density until they reach a certain potential. As can be seen, oxide layers as thin as 10 nm can be observed with grazing incidence microspectroscopy. Although this particular experiment did not require **micro**-spectroscopic methods, future plans include microscopic imaging of oxide (and other) films on metal surfaces including Al, Ta, and Zr.

Ideally, *in situ* grazing incidence micro-spectroscopy is planned, where oxide films are probed through a thin electrolyte layer above the metal surface.

Figure 6. Grazing incidence microspectra of thin oxide layers on an aluminum surface.

SYNCHROTRON INFRARED FACILITIES WORLDWIDE

Facilities for IR synchrotron radiation can be found throughout the world, serving to produce light for the scientific community. The National Synchrotron Light Source (NSLS, Brookhaven National Laboratory) presently operates six IR beamlines, with four IR microscopes (Beamlines U2A, U2B, U4-IR, and U10B), making it a premier synchrotron facility for IR investigations (Carr et al., 1998). Active IR beamlines can also be found at UVSOR, Okasaki (Japan); ALS, Berkeley and SRC, Stoughton (USA). In Europe, IR activities continue at the SRS, Daresbury (UK); LURE, Orsay (France); MAXLAB, Lund (Sweden); and at Dapne, Frascati (Italy). Other facilities that are either planning or considering IR programs include Diamond, Rutherford Lab (UK); BESSY II, Berlin, ANKA, Karlsruhe and DELTA, Dortmund (Germany); Duke-FEL, Durham (USA); CLS, Saskatoon (Canada); LNLS, Campinas, (Brazil); CAMD, Baton Rouge, (USA); SURF-3, Gaithersburg (USA); NSRL, Hefei (China); SPring8, Nishi-Harima (Japan); and SRRC, Hsinchu (Taiwan). Based on the increasing interest in synchrotron IR radiation, it is clear that the application of synchrotron IR spectroscopy to multidisciplinary problems has a bright future.

USEFUL WEBSITES AND VENDORS FOR IR MICROSPECTROSCOPY

INFRARED HOMEPAGE AT THE NSLS:
http://infrared.nsls.bnl.gov

IR MICROSCOPES
Bruker: http://www.brukeroptics.com
Biorad: http://www.bio-rad.com
Perkin Elmer: http://instruments.perkinelmer.com
Thermo Nicolet: http://www.nicolet.com

IR TRANSPARENT SUBSTRATES
International Crystal Laboratories:
http://www.icmfg.com/
ISP Optics:
http://www.ispoptics.com/
McCarthy Scientific:
http://www.mccarthyscientific.com/
Spectral Systems:
no website, phone: (845) 896-2200
Spectra Tech:
http://www.spectra-tech.com/

IR REFLECTIVE SUBSTRATES
Kevley Technologies:
no website, phone: (440) 842-6892

DATA ANALYSIS SOFTWARE
Thermo Nicolet:
http://www.nicolet.com
Bruker:
http://www.brukeroptics.com
Spectral Dimensions:
http://www.spectraldimensions.com/
Cytospec:
http://www.cytospec.com/
Galactic:
http://www.galactic.com/

WORKS CITED

Byler, D. M., and H. Susi. 1986. Examination of the secondary structure of proteins by deconvolved FTIR spectra. *Biopolymers.* 25:469-87.

Carr, G. L., P. Dumas, C. J. Hirschmugl, and G. P. Williams. 1998. Infrared Programs at the National Synchrotron Light Source. *Nuovo Cimento.* 20D:375.

Carr, G. L., J. A. Reffner, and G. P. Williams. 1995. Performance of an infrared microspectrometer at the NSLS. *Rev. Sci. Instr.* 66:1490-1492.

Carr, G. L., and G. P. Williams. 1997. Infrared microspectroscopy with synchrotron radiation. *SPIE Conf. Proc.* 3153:51-59.

Chyan, O. M. R., J. J. Chen, F. Xu, and J. Wu. 1997a. subject: IRMS and microelectronics. *Anal. Chem.* 69:2434-2437.

Chyan, O. M. R., J. Wu, and J. J. Chen. 1997b. subject: IRMS and semiconductors. *Appl. Spec.* 51:1905-1909.

Colarusso, P., L. H. Kidder, I. W. Levin, J. C. Fraser, J. F. Arens, and E. N. Lewis. 1998. Infrared spectroscopic imaging: From planetary to cellular systems. *Applied Spectr.* 52:106A.

Duncan, W., and G. P. Williams. 1983. *Applied Optics.* 22:2914.

Fogarassy, E., A. Slauoi, C. Fuchs, and J. L. Regolini. 1987. *Appl. Phys. Lett.* 51:337.

Jackson, M., and H. H. Mantsch. 1999. Ex vivo tissue analysis by infrared microspectroscopy. *In* International Encyclopedia of Vibrational Spectroscopy.

Lewis, E. N., P. J. Treado, R. C. Reeder, G. M. Story, A. E. Dowrrey, C. Marcott, and I. W. Levin. 1995. Fourier transform spectroscopic imaging using an infrared focal-plane array detector. *Anal. Chem.* 67:3377.

Reffner, J. A., P. A. Martoglio, and G. P. Williams. 1995. Fourier Transform Infrared Microscopical Analysis with Synchrotron Radiation: The Microscope Optics and System Performance. *Rev. Sci. Instr.* 66:1298.

Susi, H., and D. M. Byler. 1983. Protein structure by Fourier transform infrared spectroscopy: second derivative spectra. *Biochem Biophys Res Commun.* 115:391-7.

REPRESENTATIVE PUBLICATIONS

Bantignies, J.L., G. L. Carr, D. Lutz, S. Marull, G. P. Williams, and G.Fuchs. Organic reagent interaction with hair spatially characterized by infrared microspectroscopy using synchrotron radiation. *Int. J. Cosmet. Science* **20** 381 (1998).

Bantignies, J.L., G.L. Carr, P. Dumas, L.M. Miller, G.P. Williams. Applications of Infrared Microspectroscopy to Geology, Biology, and Cosmetics. *Synchrotron Radiation News*, **11**, 31-36 (1998).

Bradley, J.P., L.P. Keller, T.P. Snow, M.S. Hanner, G.J. Flynn, J.C. Gezo, S.J. Clemett, D.E. Brownlee, J.E. Bowey. An Infrared Spectral Match Between GEMS and Interstellar Grains. *Science*, **285**, 1716-1718 (1999).

Carr, G. L., P. Dumas, C. J. Hirschmugl, and G. P. Williams. Infrared Programs at the National Synchrotron Light Source. *Nuovo Cimento.* **20D**, 375 (1998).

Carr, G.L. Resolution limits for infrared microspectroscopy explored with synchrotron radiation. *Rev. Sci. Instr.*, **72**, 1613-1619 (2001).

Carr, G.L. High-resolution microspectroscopy and sub-nanosecond time-resolved spectroscopy with the synchrotron infrared source. *Vibrational Spectroscopy*, **19**, 53-60 (1999).

Carr, G.L., J.A. Reffner, G.P. Williams. Performance of an infrared microspectrometer at the NSLS. *Rev. Sci. Instr.* **66,** 1490-92 (1995).

Choo, L. P., D. L. Wetzel, W. C. Halliday, M. Jackson, S. M. LeVine, and H. H. Mantsch. In situ characterization of beta-amyloid in Alzheimer's diseased tissue by synchrotron Fourier transform infrared microspectroscopy. *Biophys J.* **71**, 1672-9 (1996).

Clayton, C.R. and Gary P. Halada, Zairyo-To-Kankyo. The Application of Laboratory and Synchrotron-based Spectroscopic Techniques to the Study of Passive Films and Corrosion Protective Layers. *Corrosion Engineering,* **50**, 364-372 (2001)

Ghosh, U., R. G. Luthy, J. Seb Gillette and R. N. Zare. Microscale Location, Characterization, and Association of Polycyclic Aromatic Hydrocarbons on Harbor Sediment Particles. *Environmental Science & Techn.,* **34**, 1729-36 (2000).

Goncharov, A. F., V. V. Struzhkin, H. K. Mao, and R. J. Hemley. Raman spectroscopy of dense H_2O and the transition to symmetric hydrogen bonds. *Phys. Rev. Lett.*, **83**, 1998-2001 (1999).

Goncharov, A.F., E. Gregoryanz, H. K. Mao, Z. Liu, and R. J. Hemley. Optical evidence for a nonmolecular phase of nitrogen above 150 GPa. *Phys. Rev. Lett*. **85**, 1262-1265 (2000).

Gregoryanz, E. A. F. Goncharov, R. J. Hemley, and H. K. Mao. High-pressure amorphous nitrogen. *Phys. Rev. B*, **64**, 052103-1 (2001).

Guilhaumou, N., P. Dumas, G.L.Carr and G.P.Williams. Synchrotron Infrared Microspectrometry applied to Petrography in micron scale range, Fluid chemical analysis and mapping. *Applied Spectroscopy* **52**, 1029 (1998).

Hemley, R. J. and H. K. Mao. Progress in cryocrystals to megabar pressures. *J. Low Temp. Phys.*, **122**, 331-344 (2001).

Hemley, R. J. Effects of high pressure on molecules. *Ann. Rev. Phys. Chem*., **51**, 763-800 (2000).

Hemley, R. J., H. K. Mao, and S. A. Gramsch. Pressure-induced transformations in deep mantle and core minerals. *Min. Mag.*, **64**, 157-184 (2000).

Huang, R., L.M. Miller, C.S. Carlson, M.R. Chance. FTIR Analysis of Tibia Bone From Ovariectomized Cynomolgus Monkeys (*Macaca fascicalaris)* and the Effect of Nandrolone Decanoate Treatment. *Bone*, **30**, 492-497 (2002).

Jamin, N., P. Dumas, J. Moncuit, W.H. Fridman, J.-L. Teillaud, G.L. Carr and G.P. Williams. Chemical Imaging of Nucleic Acids, Proteins and Lipids of a Single Living Cell. Application of Synchrotron Infrared Microspectrometry in Cell Biology. *Cellular and Molecular Biology* **44**, 9 (1998).

Jamin, N., P. Dumas, J. Moncuit, W.H. Fridman, J.-L. Teillaud, G.L. Carr and G.P. Williams. Highly resolved Chemical Imaging of Living Cells by using Synchrotron Infrared Microspectrometry. *PNAS*, **95,** 4837 (1998).

Kagi, H., R. Lu, P. Davidson, A. Goncharov, H. K. Mao, R. J. Hemley. Evidence for ice VI as an inclusion of cuboid diamonds from high *P-T* near infrared spectroscopy. *Min. Mag*., **64***,* 1089 (2000).

Kagi, H., R. Lu, P. M. Davidson, A. F. Goncharov, H. K. Mao, and R. J. Hemley. Evidence for ice VI as an inclusion of cuboid diamonds from high *P-T* near infrared spectroscopy. *Min. Mag*., **64***,* 1089-1097 (2000).

Keller, L.P., S. Hony, J.P. Bradley, F.J. Molster, L.B.F.M. Waters, J. Bouwman, A. de Koter, D.E. Brownlee, G.J. Flynn, T. Henning, H. Mutschke. Identification of iron sulfide grains in protoplanetary disks. *Nature*, **417**, 148-50 (2002).

Marinkovic, N.S., A.R. Adzic, M. Sullivan, K. Kovac, L.M. Miller, D.L. Rousseau, S.R. Yeh, M.R. Chance. Design and implementation of a rapid-mixer flow cell for time-resolved infrared micro-spectroscopy. *Rev. Sci. Instr.*, **71**, 4057-60 (2000).

Miller, L.M., T.J. Tague. Development and biomedical applications of fluorescence-assisted synchrotron infrared microspectroscopy. *Vibrational Spectroscopy*, **849**, 1-7 (2002).

Miller, L.M., C.S. Carlson, D. Hamerman, M.R. Chance. Chemical Differences in Subchondral Osteoarthritic Bone Observed with Synchrotron Infrared Microspectroscopy. *Bone*, **23**, S458 (1999).

Miller, L.M., C.S. Carlson, G.L. Carr, M.R. Chance. A Method for Examining the Chemical Basis for Bone Disease: Synchrotron Infrared Microspectroscopy*. Cellular and Molecular Biology*, **44**, 117-128 (1998).

Miller, L.M., G.L. Carr, M. Jackson, G.P. Williams, P. Dumas. The impact of infrared synchrotron radiation on biology: Past, present, and future. *Synchrotron Radiation News*, **13**, 31-37 (2000).

Miller, L.M., J. Tibrewala, C.S. Carlson. Examination of Bone Chemical Composition in Osteoporosis Using Fluorescence-Assisted Synchrotron Infrared Microspectroscopy. *Cellular and Molecular Biology*, **46**, 1035-44 (2000).

Miller, L.M., P. Dumas, N. Jamin, J.-L. Teillaud, J. Miklossy, L. Forro. Combining IR spectroscopy and fluorescence imaging in a single microscope: Biomedical applications using a synchrotron infrared source. *Rev. Sci. Instr.*, **73**, 1357-60 (2002).

Miller, L.M., V. Vairavamurthy, M.R. Chance, E.P. Paschalis, F. Betts, A.L. Boskey, R. Mendelsohn. *In Situ* Analysis of Mineral Crystal Size and Phosphate Environment in Bone using Infrared Microspectroscopy of the $nu_4PO_4^{3-}$ Vibration. *Biochim. Biophys. Acta*, **1527**, 11-19 (2000).

Reffner, J. A., P. A. Martoglio, and G. P. Williams. Fourier Transform Infrared Microscopical Analysis with Synchrotron Radiation: The Microscope Optics and System Performance. *Rev. Sci. Instr.* 66:1298 (1995).

Somayazulu, M., A. Madduri, A.F. Goncharov, O. Tschauner, P.F. McMillan, H.K. Mao, and R.J. Hemley. Novel broken symmetry phase from N_2O at high pressure and high temperatures. *Phys. Rev. Lett.* **87**, 135504-1 (2001).

Struzhkin, V. V., A. F. Goncharov, H. K. Mao, R. J. Hemley, S. W. Moore, J. M. Graybeal, J. Sarrao, and Z. Fisk. Coupled magnon-phonon excitations in Sr2CuCl2O2 at high pressure. *Phys. Rev. B*, **62**, 3895-3899 (2000).

Tague, T.J., L.M. Miller, Novel Use of Fluorescence Illumination with an Infrared Microscope. *Microscopy Today*, **2**, 26-32 (2000).

Wetzel, D. L., and S. M. LeVine. Imaging molecular chemistry with infrared microscopy. *Science,* **285**, 1224 (1999).